

Supplementary Information for

# A radical mechanism for C–H bonds cross-coupling and N<sub>2</sub> activation catalysed by $\beta$ -diketiminato iron complexes

## Contents

<b>Table S1.</b> Absolute and relative electronic energies of <b>3</b> and <b>TS<sub>3,4</sub></b> calculated by using different functionals.	<b>S2</b>
<b>Table S2.</b> Absolute and relative free energies of intermediates with different spin states.	<b>S3</b>
<b>Table S3.</b> Absolute electronic energies of different spin states intermediates <b>4</b> calculated by using different functionals.	<b>S4</b>
<b>Table S4.</b> The molecular orbital compositions of <b>7</b> and <b>8</b> .	<b>S5</b>
<b>Figure S1-S2</b> Optimized structures with atom labels.	<b>S6</b>
<b>Table S5.</b> Calculated Mössbauer parameters for <b>4</b> .	<b>S7</b>

## Evaluation of density functionals

To examine the reliability of density functionals for this Fe system, we also calculated the relative electronic energies between **3** and **TS<sub>3,4</sub>** using seven others well recognized and widely used density functionals with different percentages of Hartree-Fock exchanges, including BP86<sup>1</sup>, PBE<sup>2</sup>,  $\omega$ B97X-D<sup>3</sup>,  $\omega$ B97X<sup>4</sup>, HSE06<sup>5</sup>, B3PW91<sup>6</sup> and PBEh1PBE<sup>7</sup>. The calculated relative electronic energies are listed in Table S1. All structures were calculated using the above functionals with the same basis set BS2 described in computation details. We can see that the difference of all functionals is less than 5.0 kcal mol<sup>-1</sup>, which indicates that the calculated free energy barrier of this iron catalysed nitrogen fixation and activation reaction has a very weak dependence of density functionals. More importantly, the total free energy barrier calculated by using the TPSS-D3 functional matches well with the experimental conditions. Therefore, we believe TPSS-D3 is a suitable functional for the computational study of this Fe system.

**Table S1.** Absolute and relative electronic energies of **3** and **TS<sub>3,4</sub>** calculated by using different functionals.

Functionals	<i>E</i> (Hartree)		$\Delta E$ (kcal mol <sup>-1</sup> )
	<b>3</b>	<b>TS<sub>3,4</sub></b>	<b>3</b> $\rightarrow$ <b>TS<sub>3,4</sub></b>
BP86	-3353.115309	-3353.082265	20.7
PBE	-3350.157654	-3350.122161	22.3
$\omega$ B97X-D	-3352.357423	-3352.319474	23.8
$\omega$ B97X	-3352.43285	-3352.393887	24.4
HSE06	-3350.515354	-3350.475769	24.8
B3PW91	-3352.122855	-3352.082839	25.1
PBEh1PBE	-3350.558617	-3350.517961	25.5

## Evaluation of spin states

To ensure a reliable evaluation of the proposed reaction mechanism and find out the change of spin states in the reaction, we examined the relative free energies of all intermediates at different spin-states using the same computational methods described in the text. The calculation results are listed in Table S2. All structures were optimized individually at different spin-states. The structures reported in the text are the spin-states with lower relative free energies. We can see there are some spin-crossovers along the reaction pathways. The triplet and quintet states of **4** and **12** are very close and may exist simultaneously in the reaction. Most quartet states are much more stable than sextet states except for intermediate **14**.

**Table S2.** Absolute and relative free energies of intermediates with different spin states.

Complexes	G (Hartree)		$\Delta G$ (kcal mol <sup>-1</sup> )
	Triplet	Quintet	Triplet → Quintet
<b>3</b>	-3352.086268	-3352.045499	25.6
<b>4</b>	-3352.086497	-3352.080853	3.5
<b>5</b>	-2420.725539	-2420.717106	5.3
<b>9</b>	-2938.902076	-2938.879568	14.1
<b>10</b>	-3361.593853	-3361.574942	11.9
<b>11</b>	-4292.945100	-4292.926907	11.4
<b>12</b>	-3348.020192	-3348.025917	-3.6
<b>13</b>	-3348.036748	-3348.051644	-9.3
<b>14</b>	-3757.201646	-3757.215195	-8.5
<b>16</b>	-2884.081956	-2884.090960	-5.7

Complexes	G (Hartree)		$\Delta G$ (kcal mol <sup>-1</sup> )
	Quartet	Sextet	Quartet → Sextet
<b>1</b>	-3133.334052	-3133.295239	24.4
<b>2</b>	-2420.660457	-2420.600978	37.3
<b>4'</b>	-2420.629091	-2420.609538	12.3
<b>6</b>	-3352.125426	-3352.101403	15.1
<b>7</b>	-2420.126325	-2420.098744	17.3
<b>8</b>	-2529.701080	-2529.647555	33.6
<b>15</b>	-2474.828032	-2474.810354	11.1
<b>17</b>	-3293.282627	-3293.261400	13.3
<b>18</b>	-3293.280899	-3293.233359	29.8

Since our calculations indicate that **4** has a triplet ground state, which is different with the results in ref. 31 in the text, we further evaluated the influence of density functionals to the electronic energy calculations results of **4**. Table S3 lists the triplet and quintet state energies of **4** obtained by using five other functionals  $\omega$ B97X-D,<sup>3</sup> B3LYP-D3,<sup>8</sup> TPSS-h,<sup>9</sup> PBE,<sup>2</sup> and BP86.<sup>1</sup> We can see that  $\omega$ B97X-D, B3LYP-D3 and TPSS-h functionals gave more stable quintet states, but PBE, BP86 and TPSS-D3 gave more stable triplet states. Such results indicates that the ground state of **4** has a strong spin contamination and very likely to have both triplet and quintet in the reaction.

**Table S3.** Absolute electronic energies of different spin states intermediate **4** calculated by using different functionals.

Functionals	<i>E</i> (Hartree)		$\Delta E$ (kcal mol <sup>-1</sup> )
	Triplet	Quintet	Triplet $\rightarrow$ Quintet
$\omega$ B97X-D	-3351.725786	-3351.736223	-6.5
B3LYP-D3	-3352.462258	-3352.469404	-4.5
TPSS-h	-3352.433736	-3352.438482	-3.0
PBE	-3349.476750	-3349.471861	3.1
BP86	-3352.417756	-3352.411683	3.8
TPSS-D3	-3352.806456	-3352.796732	6.1

**Table S4.** The molecular orbital compositions of **7** and **8**.

Molecule	Orbit	The contributions of atomic orbitals						
7	β-114	1(Fe)	13(C)	26(C)				
		3d <sub>xz</sub>	2p <sub>z</sub>	2p <sub>z</sub>				
		68.64%	11.84%	11.83%				
	β-115	1(Fe)	24(C)	11(C)	41(C)	2(N)	3(N)	18(C)
		3d <sub>yz</sub>	2p <sub>z</sub>	2p <sub>z</sub>	2p <sub>z</sub>	2p <sub>z</sub>	2p <sub>z</sub>	2p <sub>z</sub>
		73.36%	6.68%	4.74%	4.74%	2.23%	2.11%	2.07%
8	β-121	1(Fe)	3(N)	1(Fe)	13(C)	10(C)	2(N)	
		3d <sub>xz</sub>	2p <sub>x</sub>	3d <sub>xy</sub>	2p <sub>z</sub>	2p <sub>z</sub>	2p <sub>x</sub>	
		61.83%	13.78%	9.17%	3.51%	3.49%	2.47%	
	β-122	1(Fe)	3(N)	1(Fe)	2(N)	41(C)	37(C)	45(C)
		3d <sub>yz</sub>	2p <sub>y</sub>	3d <sub>x<sup>2</sup>-y<sup>2</sup></sub>	2p <sub>y</sub>	2p <sub>z</sub>	2p <sub>z</sub>	2p <sub>z</sub>
		54.44%	13.67%	11.70%	2.90%	2.86%	2.54%	2.51%

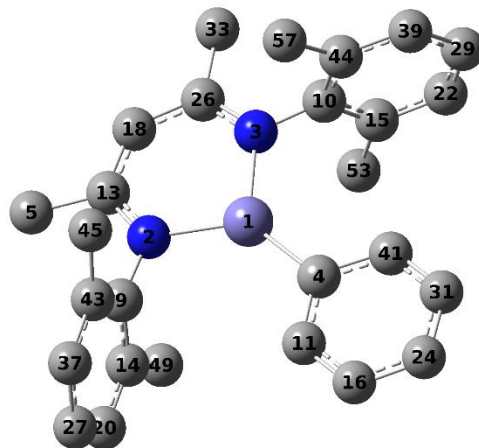


**Figure S1.** Optimized structure and atom labels of **7**. Hydrogen atoms are omitted for clarity.

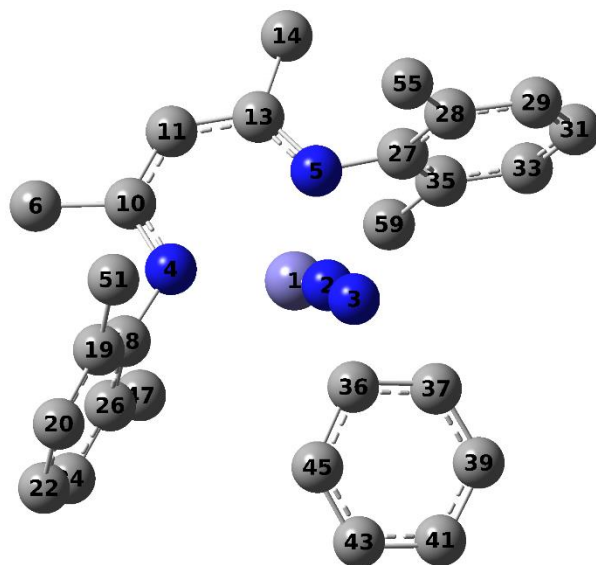


**Figure S2.** Optimized structure and atom labels of **8**. Hydrogen atoms are omitted for clarity.

## The prediction of Fe Mössbauer parameters for **4**

The Mössbauer parameters of **4** were calculated by using the ORCA program package, version 4.0.0<sup>8</sup> for five functionals B3LYP-D3,<sup>9</sup> TPSS-D3<sup>10</sup>, M06,<sup>11</sup> M06-L,<sup>11</sup> and CAM-B3LYP,<sup>12</sup> with a combination of the CP(PPP) basis set for iron and def2-TZVP for all other atoms. Resolution of identity was used to approximate COSX integrals. We can see that the B3LYP-D3, TPSS-D3, and CAM-B3LYP functionals have quintet state  $|\Delta E_Q|$  results closer to the experimental value, while the M06 and M06-L functionals have triplet state  $|\Delta E_Q|$  results slightly closer to the experimental value. The isomer shifts  $\delta$  were obtained using the extended calibration parameters reported by Neese.<sup>13-15</sup> M06, M06L and CAM-B3LYP do not have such calibration parameters available so we used the calibration parameters for B3LYP. We can see that the  $\delta$  values obtained from different density functionals vary significantly.

**Table S5.** Calculated Mössbauer parameters for **4**.

<b>4</b>	Expt.	Spin states	M06	M06L	B3LYP-D3	TPSS-D3	CAM-B3LYP
$ \Delta E_Q $ (mm/s)	3.08	Triplet	3.36	3.21	2.47	1.98	2.66
		Quintet	2.81	2.62	3.07	2.71	3.26
$\delta$ (mm/s)	0.54	Triplet	5.70	9.70	-59.8	0.07	-56.42
		Quintet	5.75	9.80	0.15	0.21	-1.40

## References

- (1) (a) A. D. Becke, *Phys. Rev. A*, 1988, **93**, 3098. (b) J. P. Perdew, *Phys. Rev. B*, 1986, **33**, 8822.
- (2) (a) J. P. Perdew, K. Burke, M. Ernzerhof, *Phys. Rev. Lett.*, 1996, **77**, 3865. (b) J. P. Perdew, K. Burke, M. Ernzerhof, *Phys. Rev. Lett. M.*, 1997, **78**, 1396.
- (3) J.D. Chai, M. Head-Gordon, *Phys. Chem. Chem. Phys.*, 2008, **10**, 6615-6620.
- (4) J.D. Chai, M. Head-Gordon, *J. Chem. Phys.*, 2008, **128**, 084106.
- (5) (a) T. M. Henderson, A. F. Izmaylov, G. Scalmani, G. E. Scuseria, *J. Chem. Phys.*, 2009, **131**, 044108. (b) A. V. Krukau, O. A. Vydrov, A. F. Izmaylov, G. E. Scuseria, *J. Chem. Phys.*, 2006, **125**, 224106.
- (6) (a) J. P. Perdew, J. A. Chevary, S. H. Vosko, K. A. Jackson, M. R. Pederson, D. J. Singh, C. Fiolhais, *Phys. Rev. B.*, 1993, **48**, 4978-4978. (b) J. P. Perdew, J. A. Chevary, S. H. Vosko, K. A. Jackson, M. R. Pederson, D. J. Singh, C. Fiolhais, *Phys. Rev. B.*, 1992, **46**, 6671-6687.
- (7) M. Ernzerhof, J. P. Perdew, *J. Chem. Phys.*, 1998, **109**, 3313-3320.
- (8) F. Neese, *ORCA*, version 4.0; Max-Planck-Institut für Bioanorganische Chemie: Mülheim an der Ruhr, Germany, *WIREs Comput. Mol. Sci.* 2018, **8**, e1327.
- (9) (a) A. D. Becke, *J. Chem. Phys.*, 1993, **98**, 5648-5652. (b) S. Grimme, J. Antony, S. Ehrlich, H. Krieg, *J. Chem. Phys.*, 2010, **132**, 154104.
- (10)(a) J. Tao, J. P. Perdew, V. N. Staroverov and G. E. Scuseria, *Phys. Rev. Lett.*, 2003, **91**, 146401-146601. (b) V. N. Staroverov, G. E. Scuseria, J. M. Tao and J. P. Perdew, *J. Chem. Phys.*, 2003, **119**, 12129-12137.
- (11)Y. Zhao, D. G. Truhlar, *Theor. Chem. Acc.*, 2008, **120**, 215-241.
- (12)T. Yanai, D. Tew, N. Handy, *Chem. Phys. Lett.*, 2004, **393**, 51-57.
- (13)F. Neese, *Inorg. Chim. Acta*, 2002, **337**, 181-192.
- (14)M. Römel't, S. Ye, F. Neese, *Inorg. Chem.*, 2009, **48**, 784-785.
- (15)S. Sinnecker, D. L. Slep, E. Bill, F. Neese, *Inorg. Chem.*, 2005, **44**, 2245.